

## M.4. Clonaje, expresión y purificación de las carboxipeptidasas reguladoras CPE y CPD

### M.4.1. Clonaje y expresión

#### M.4.1.1. CPE

Debido a que el sistema de expresión que se iba a utilizar era el de la levadura *Pichia pastoris*, se hacía necesario el subclonaje de los cDNAs de las carboxipeptidasas reguladoras en el vector de expresión de este sistema, denominado pPIC9. Para aumentar las posibilidades de éxito tanto en la expresión como en la posterior cristalización (el objetivo final del proyecto era la resolución de la estructura tridimensional de estas proteínas), se decidió trabajar no sólo con la forma silvestre, sino además con dos mutantes. El primer mutante escogido fue Δ23 CPE, una forma de la CPE con una delección de 23 residuos en su extremo C-terminal. La ventaja de este mutante era que, además de que conserva la actividad, tiene reducida la tendencia a agregarse que presenta la CPE silvestre (Varlamov y Fricker, 1996), lo cual debía facilitar enormemente su expresión extracelular. El segundo mutante, E270Q CPE, es inactivo debido a una mutación puntual en el residuo 270 pero conserva su capacidad de unión al sustrato. Se escogió este mutante pensando en un posible co-cristal enzima-sustrato.

##### M.4.1.1.1. Introducción de la diana Mlu I en pPIC 9. Diseño de un adaptador.

Los cDNAs de la CPE silvestre, la CPE truncada y el mutante nos fueron proporcionados por el Dr. LD Fricker, de Albert Einstein College of Medicine of the Yeshiva University (Nueva York) y se encontraban en unos vectores derivados del vector de expresión de Baculovirus pVL1393 llamados pCPE20, pCPE53 y pCPE64,

respectivamente. Estos cDNAs estaban flanqueados por las dianas *Mlu* I en el extremo 5' y *Not* I en el extremo 3'.

El vector de expresión de *Pichia pastoris* en el que se querían subclonar los cDNAs, pPIC 9, posee una diana de restricción *Not* I en el policonector, pero no la diana *Mlu* I. El primer objetivo a conseguir fue, por tanto, la introducción de este lugar de corte en el vector pPIC 9. Para ello, se diseñó un adaptador oligomérico de DNA que contenía el lugar de corte para *Mlu* I y unos extremos cohesivos simulando una restricción con *Xho* I y *Eco* RI. pPIC 9 contiene las dianas *Xho* I y *Eco* RI en su sitio para clonaciones.

Las dos secuencias oligoméricas que tenían que formar el adaptador fueron sintetizadas por una casa comercial y fueron sometidas posteriormente en el laboratorio a una reacción de hibridación. Luego, se fosforiló el adaptador con una quinasa.

Por otro lado, se digirió pPIC 9 con las enzimas *Xho* I y *Eco* RI, y se recortó la banda de gel de agarosa correspondiente a 8,0 kb. Se extrajo el DNA y se defosforilaron los extremos. Entonces se procedió a la ligación del adaptador a pPIC 9 y se obtuvo un vector modificado de pPIC 9 al que se denominó pPIC 9-*Mlu* I (véase figura M.4).

#### **M.4.1.1.2. Introducción de los cDNAs en el vector pPIC 9 modificado**

Los vectores pCPE 20, pCPE 53 y pCPE 64, que contenían los cDNAs a clonar, se digirieron con las enzimas *Mlu* I y *Not* I. Esta restricción generó unos insertos de 1,7 kb en los casos de la CPE silvestre y del mutante E270Q y un inserto de 1,5 kb en el caso de la CPE truncada. Las bandas correspondientes a estos insertos se recortaron del gel de agarosa y se purificó el DNA.

El vector pPIC 9-*Mlu* I también se digirió con las mismas enzimas de restricción, se purificó el DNA de la banda de 8,0 kb y se defosforilaron sus extremos. A continuación, se ligaron los tres insertos al vector y se transformaron células competentes de *E. coli* de la cepa JM83.

Como resultado, se obtuvieron tres construcciones con los cDNAs de la CPE silvestre, la CPE truncada y el mutante E270Q clonados en un vector de expresión de *P. pastoris*. Las llamamos, respectivamente, pCPE 88, pCPE 87 y pCPE 89 (véase figura M.4). Las tres construcciones fueron secuenciadas de forma automática para comprobar que el subclonaje se había llevado a cabo correctamente.

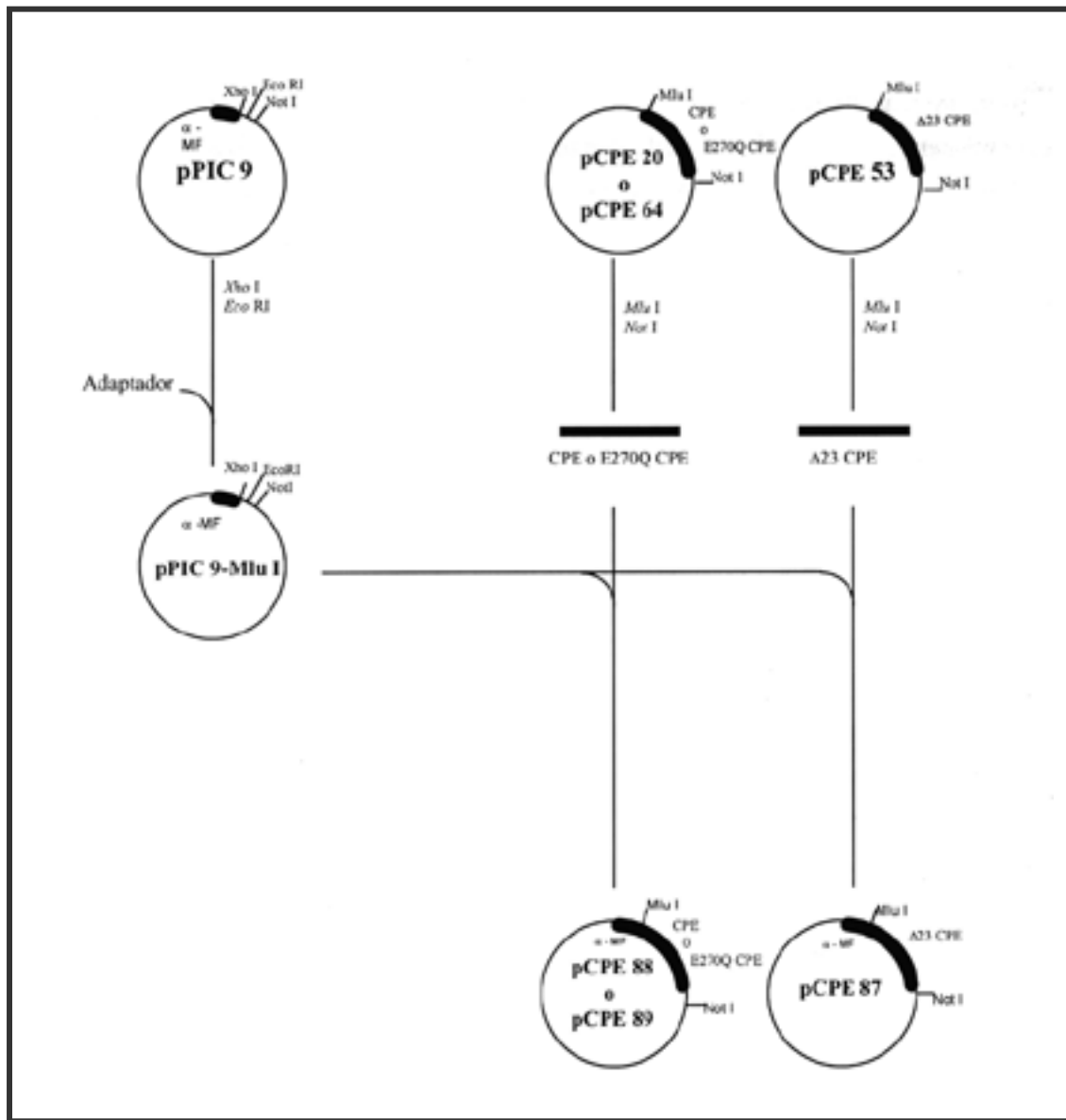


**Figura M.4. Clonaje de los cDNAs de la CPE silvestre y dos formas mutadas.**

#### M.4.1.1.3. Transformación de *P. pastoris* y expresión

Se procedió a la transformación de *P. pastoris* tal y como se describe en el apartado M.1.2.10. El DNA a introducir se linealizó con la enzima *Sal I*, que tiene una única diana de restricción en pPIC 9.

El proceso de expresión consta de dos etapas: un primer paso en que se cultiva la levadura transformada en medio rico BMGY, que tiene glicerol como fuente de carbono

y está tamponado a pH 6, y un segundo paso en el que el medio de cultivo es sustituido por BMMY, que contiene metanol en vez de glicerol, de manera que se induce la expresión de la proteína recombinante. La expresión se realizó en un volumen de 1 litro en la primera etapa de crecimiento de la levadura y luego se concentró a 200 ml para la etapa de inducción de la expresión. El paso de concentración se puede realizar gracias a que *P. pastoris* es capaz de crecer a densidades celulares muy altas ( $DO_{660} = 15-20$ ). Suele ser conveniente hacer crecer la levadura durante dos días y luego mantener la inducción durante tres días. El medio de cultivo BMMY contiene un 1% de metanol y se tiene que añadir cada día un 1% de metanol al cultivo para mantener la inducción.

### M.4.1.2. CPD

#### M.4.1.2.1. Clonaje en el vector de expresión de *Pichia pastoris*

Se disponía de un vector (de expresión en Baculovirus) llamado p180x que contiene los dominios 1 y 2 de CPD de pato. Lo que se deseaba clonar era el dominio 2. En el extremo 3' del cDNA del dominio 2 se encuentra la diana de restricción *Stu* I y a unos 150 pb del extremo 5' se encuentra la diana *Sna* BI. Ambas enzimas de restricción, *Stu* I y *Sna* BI, generan extremos romos. pPIC 9, el vector en el que se quería clonar el dominio 2 de CPD, también contiene la diana *Sna* BI. La estrategia de clonaje constaba de dos pasos: en el primer paso, se digirió el vector pPIC 9 con *Sna* BI y se defosforilaron sus extremos. Aparte, se digirió p180x con *Stu* I y *Sna* BI y se purificó el inserto generado de 1,2 kb a partir de un gel de agarosa. Con el vector y el inserto obtenidos, se procedió a su ligación y con el producto se transformó *E. coli*. Se eligió uno de los clones con el inserto en la orientación correcta para el segundo paso de la estrategia. A este vector se le llamó pPIC 9-SS.

Con este primer paso, se había clonado la mayor parte del cDNA del dominio 2 de CPD en pPIC 9 (véase figura M.5), pero no los 150 pb de su extremo 5'. El segundo paso de clonaje consistió en amplificar el fragmento que faltaba mediante PCR. Para realizar esta PCR se diseñaron unos cebadores que se denominaron DOM2NH-F para el extremo 5' y DUCK1681-R para el extremo 3'. DOM2NH-F, de 46 nucleótidos de largo, contiene la diana de restricción *Xho* I, la secuencia que codifica para la señal de procesamiento KEX2 y los 22 nucleótidos del extremo 5' del dominio 2 de CPD.

DUCK1681-R, de 21 nucleótidos, corresponde a una zona 50 pb "downstream" de la diana *Sna* BI que contiene el cDNA del dominio 2 de CPD. Como molde de DNA para la PCR, se usó el vector p180x. El producto obtenido se cortó por los extremos con las enzimas *Xho* I y *Sna* BI. Este fragmento se ligó con el vector pPIC 9-SS, previamente digerido también con las enzimas *Xho* I y *Sna* BI y el producto se transformó a *E. coli*. Como resultado, se obtuvo el cDNA del dominio 2 de CPD insertado en el vector de expresión de *Pichia pastoris* pPIC 9. A este vector se le denominó pPIC 9-D1-x. Se secuenció de forma automática y se comprobó que no había habido ningún error en el proceso de clonaje.

#### **M.4.1.2.2. Transformación de *P. pastoris* y expresión**

A continuación se procedió a la transformación de *P. pastoris* con la construcción obtenida y a la expresión de la proteína recombinante de la misma manera que la anteriormente descrita para la CPE (véase M.4.1.1.3).

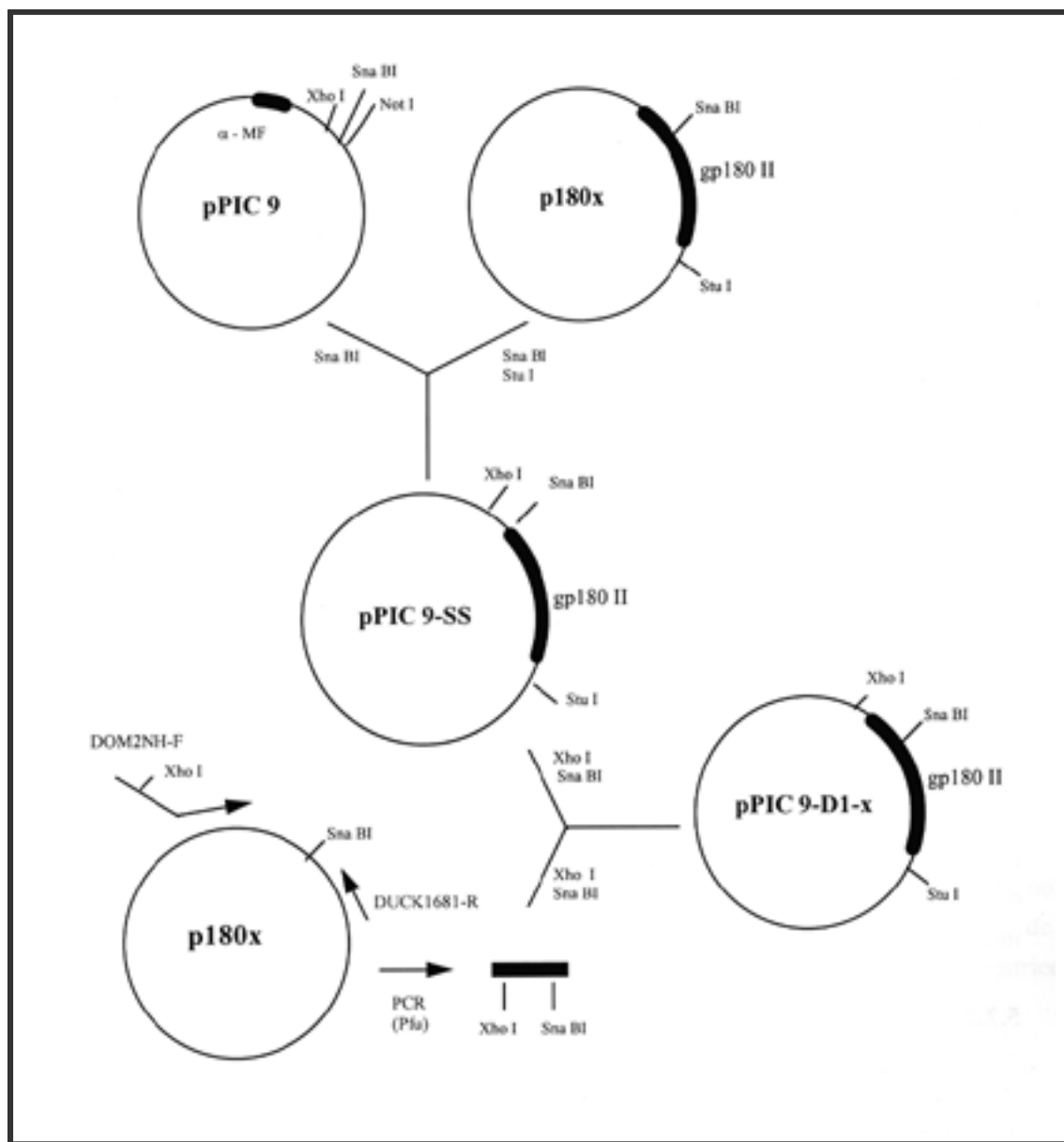


**Figura M.5. Clonaje del dominio 2 de CPD en el vector de expresión de *P. pastoris* pPIC 9.**

## M.4.2. Purificación de las carboxipeptidasas reguladoras CPE y CPD

Para la purificación de las carboxipeptidasas reguladoras CPE y CPD se ha utilizado una columna de afinidad de 0.7 ml de *p*-aminobenzoil-Arg sefarosa 6B.

El protocolo de purificación (Fricker, 1995) se detalla a continuación:

- 1.- Antes de introducir la muestra, se prepara la columna haciendo pasar por ella 40 ml de ácido acético al 5% y 100 ml de tampón de lavado.

Tampón de lavado:

Acetato de sodio	0,1 M
Cloruro de sodio	1 M
Triton x100	1%

- 2.- Se centrifuga el medio de cultivo con las células productoras de *Pichia pastoris* a 15700 x g.
- 3.- Se descarta el pellet y se añade al sobrenadante 1/10 (volumen) de acetato de sodio 1M pH 5,5. Se ha de acabar de ajustar el pH final a 5,5.
- 4.- Se añade un volumen de agua MilliQ. En este punto es conveniente guardar 1 ml de la muestra para posterior análisis electroforético y de actividad.
- 5.- Se aplica la muestra a la columna y se recicla el eluido de 2 a 3 veces.
- 6.- Se lava la columna con al menos un volumen de la muestra de tampón de lavado. En ningún caso menos de 200 ml.
- 7.- Se enjuaga la columna con 20 ml de acetato sódico 10 mM pH 5,5.
- 8.- Se eluye con el tampón de elución correspondiente para CPE o CPD en tres tandas de 15 ml.

Tampones de elución:

Para CPE:	Tris-HCl	50 mM
	Cloruro sódico	100 mM
	Triton x100	0,01% pH 8,0

Para CPD:	Tris-HCl	50 mM
	Cloruro sódico	100 mM
	Triton x100	0,01%
	Arginina	25 mM pH 8,0

## M.5. Aparatos y reactivos

### M.5.1. Aparatos

Agitador rotativo de geles Biotron (España).

Agitador vórtex Heidolph, modelo Reax 2000 (Alemania).

Agitadores magnéticos SBS, modelo A-03.

Autoclaves Autester-E y Autester 437-P de JP Selecta (España).

Balanzas Mettler AJ100, PJ300 y H64 (Alemania).

Baño termostático JP Selecta, modelo Tectron Bio-Medic 60 (España).

Bloque termostático Bioblock, modelo 92617 (Francia).

Cabina de flujo laminar Faster, modelo TWO-30 (Italia).

Cámara fotográfica Polaroid, modelo MP4 (EE.UU.)

Centrífugas Beckman modelos J2-HS y J2-21 (EE.UU.) con rotores JA20, JA14, JS13.1 y Sorvall Instruments du Pont, modelo RC5C (EE.UU.) con rotores GS-A y GS-3.

Congelador -80°C Forma Scientific, modelo 8325 (EE.UU.).

Cubeta de transferencia Bio Rad, modelo Mini Trans-Blot (EE.UU.).

Cubetas de electroforesis para geles de acrilamida Bio Rad, modelo Mini-Protean II (EE.UU.).

Cubetas de electroforesis para geles de agarosa Miniphor Submarine Electrophoresis Unit LKB, modelo 2013 (Suecia) y cubetas Pharmacia, modelos GNA-100 y GNA-200 (Suecia).

Espectrofotómetro Hewllett Packard Diode Array Spectrophotometer, modelo 8452<sup>a</sup> (EE.UU.) e Hitachi Spectrophotometer, modelo 220S (Japón).

Estufa incubadora de cultivos Sanyo, modelo Mir-152 (Japón).

Fuente de alimentación para electroforesis Hoefer Scientific Inst., modelo PS500XT (EE.UU.).

FPLC System de Pharmacia (Suecia).

HPLC Waters Photodiode Array Detector 994 (EE.UU.) con ordenador Nec SX Plus (EE.UU.).

Incubador de aire con agitación orbital Braun, modelo Certomat S (Alemania) e incubador New Brunswick, modelo Classic G25 (EE.UU.).

Microcentrífugas Eppendorf, modelo 5415C (EE.UU.), IEC, modelo Micro Max (EE.UU.) y microcentrífugas refrigeradas Sigma, modelos 2MK y 2K15 (Alemania).

PHmetro Crison Instruments S.A., modelo Micro pH 2001 (España) con un electrodo Ingold (Suiza).

Transiluminador ultravioleta Fotodyne Inc. (EE.UU.).

## M.5.2. Reactivos

Los reactivos de uso general utilizados han sido de grado analítico de las firmas Merck (Alemania), Sigma Chemical Co (EE.UU.) y Carlo Erba (Italia). La procedencia de los productos de uso más específico se indica a medida que aparecen en el texto.

## M.6. Referencias

Birnboim HC, Doly J (1979) A rapid alkaline extraction procedure for screening recombinant plasmid DNA. Nucleic Acids Res 6, 1513-1523.

Bradford MM (1976) A rapid and sensitive method for the quantitation of microgram quantities of protein utilizing the principle of protein-dye binding. Anal Biochem 72, 248-254.

Burgos FJ, Pascual R, Vendrell J, Cuchillo CM, Avilés FX (1989) The separation of pancreatic procarboxypeptidases by High Performance Liquid Chromatography and chromatofocusing. J Chromatogr 481, 233-243.

Burgos FJ, Salvà M, Villegas V, Soriano F, Méndez E, Avilés FX (1991) Analysis of the activation process of porcine procarboxypeptidase B and determination of the sequence of its activation segment. *Biochemistry* 30, 4082-4089.

Casadaban MJ, Cohen SN (1980) Analysis of gene signals by DNA fusion and cloning in *Escherichia coli*. *J Mol Biol* 138, 179-207.

Fricker LD, Snyder SH. (1982) Enkephalin convertase: purification and characterization of a specific enkephalin-synthesizing carboxypeptidase localized to adrenal chromaffin granules. *Proc Natl Acad Sci* 79, 3886-3890.

Fricker LD, Snyder SH (1983) Purification and characterization of enkephalin convertase, an enkephalin-synthesizing carboxypeptidase. *J Biol Chem* 258, 10950-10955.

Fricker LD (1995) *Methods Neurosci* 23, 237-250.

Görisch H (1988) Drop dialysis: time course of salt and protein exchange. *Anal Biochem* 173, 393-398.

Hillenkamp F, Karas M, Beavis RC, Chait BT (1991) Matrix-assisted laser desorption/ionisation mass spectrometry. *Anal Chem* 63, 1193-1203.

Laemmli, UK (1970) Cleavage of structural proteins during the assembly of the head of bacteriophage T4. *Nature* 227, 680-685.

Mandel M, Higa A (1970) Calcium-dependent bacteriophage DNA infection. *J Mol Biol* 53, 159-162.

Renart J, Reiser J, Stark GR (1979) Transfer of proteins from gels to diazobenzyloxymethyl-paper and detection with antisera: a method for studying antibody specificity and antigen structure. *Proc Nat Acad Sci* 76, 3116-3120.

Schägger H, von Jagow G (1987) Tricine-sodium dodecyl sulfate-polyacrylamide gel electrophoresis for the separation of proteins in the range from 1 to 100 kDa. *Anal Biochem* 166, 368-379.

Schwert GW, Takenaka Y (1955) Spectrometric determination of Trypsin and chymotrypsin. Biochem Biophys Acta 16, 570-576.

Towbin H, Staehelin T, Gordon J (1979) Electrophoretic transfer of proteins from acrylamide gels to nitrocellulose sheets: procedure and some applications. Proc Nat Acad Sci 76, 4350-4354.

Varlamov O, Fricker LD (1996) The C-terminal region of carboxypeptidase E involved in membrane-binding is distinct from the region involved with intracellular routing. J Biol Chem 271, 6077-6083.

Ventura S, Villegas V, Sterner J, Larson J, Vendrell J, Hershberger CL, Avilés FX (1999) Mapping the pro-region of carboxypeptidase B by protein engineering. J Biol Chem 274, 19925-19933.

Villegas V, Vendrell J, Avilés FX (1995) The activation pathway of procarboxypeptidase B from porcine pancreas: participation of the active enzyme in the proteolytic processing. Protein Science 4, 1792-1800.

# **Capítulo 1.**

## **Descripción detallada de la relación estructura/función en los mecanismos de activación/inhibición de procarboxipeptidasas**

## 1.1. Summary

The activation process of pancreatic procarboxypeptidase B (pro-CPB) that gives rise to a functional enzyme by limited proteolysis is much faster than that of procarboxypeptidase A1 (pro-CPA1). This different rate of enzymatic activation has been proposed to be caused by specific conformational features at the region that connects the globular domain of the pro-segment to the enzyme and at the contacting surfaces on both moieties. A number of mutants of the pro-segment of pro-CPB have been expressed in the methylotrophic yeast *Pichia pastoris* and from their analysis, some information has been added to the previous knowledge of the activation process of pro-CPB, based on studies of the wild type porcine pro-CPB (natural and recombinant) and previously analyzed mutant forms.

The Arg 95 tryptic target is necessary and sufficient for complete activation of pro-CPB. Either Arg 95 or Arg 93 are necessary for the activation of the proenzyme, and no proteolytic processing is observed when these targets are absent, even though an artificial target is placed in position 97, emulating a tryptic target of pro-CPA1. Replacement of the connecting segment of pro-CPB by that of pro-CPA1 through the introduction of some modifications to avoid alteration of its secondary structure renders a mutant that shows a slightly different behaviour in the activation rate from the wild-type pro-CPB, without similarity to that of pro-CPA1. Replacement of the 310 helix of pro-CPB by the corresponding sequence of pro-CPA allows the appearance of residual activity in the mutated pro-CPB, confirming the hypothesis that the interaction of this structural element with the enzyme moiety prevents the accessibility of the substrates to the active site. However, the values of intrinsic activity of the mutant are much lower than those of pro-CPA1.

## 1.2. Introduction

Pancreatic carboxypeptidases are zinc metalloenzymes involved in the hydrolysis of alimentary proteins and peptides from their C-terminal end (Neurath H, 1986). Attending to their specificity, they can be classified into two groups: the A forms (CPA) with a preference for apolar C-terminal residues and the B forms (CPB), preferentially specific for basic C-terminal residues. The tertiary structures of both forms are well known (Avilés *et al*, 1993). In porcine pancreatic secretions, the precursors of the two major forms of pancreatic carboxypeptidases, pro-CPB and pro-CPA, are found in the monomeric state, making this system suitable for comparison studies of their activation processes.

A differential feature of these proteins compared to other secretory digestive zymogens is the length of their N-terminal pro-pieces (also called pro-segments or activation segments): 94, 95 and 96 residues in pro-CPA1, pro-CPB and pro-CPA2, respectively, spanning over  $\frac{1}{4}$  of the proenzyme. These segments have a compact globular fold that determines the inhibition and activation processes of the procarboxypeptidases (Avilés *et al*, 1993; Aloy *et al*, 1998).

The three-dimensional structures of porcine pro-CPB and pro-CPA1 and human pro-CPA2 have been deduced from X-ray diffraction studies (Coll *et al*, 1991; Guasch *et al*, 1992; García-Sáez *et al*, 1997), and the solution structure of the globular domain of the pro-CPB activation segment has been derived from NMR spectroscopy (Vendrell *et al*, 1991). Sequential data show that the percentage of sequence identity between forms A1 (403 residues) and B (402 residues) forms is about 45 %, but it decreases to only 31% when the comparison is restricted to the activation segments (Burgos *et al*, 1991). Structurally, the activation segments have a high similarity, even though important local differences in their secondary structures are found. These differences could be the reason for the different behaviour of the A1 and B forms upon activation. The activation processes of porcine pancreatic pro-CPA1 and pro-CPB have been studied previously in detail (Vendrell *et al*, 1990; Villegas *et al*, 1995). Both enzymes are activated by trypsin through a proteolytic cleavage that initially gives rise to the separated enzyme and activation segment moieties. However, the generation of activity is much faster in pro-CPB than in pro-CPA. On the other hand, pro-CPB completely lacks intrinsic enzymatic activity, whereas pro-CPA is able

to catalyse the hydrolysis of small synthetic peptides (Lacko et al, 1970; Reeck et al, 1972) a fact that indicates a different degree of shielding of the active centre in both forms.

In a previous work (Ventura *et al*, 1999), the cDNA coding for porcine pro-CPB was cloned and overexpressed in the yeast *Pichia pastoris*. By site-directed mutagenesis of the different tryptic targets of pro-CPB connecting segment, it was shown that the proteolytic activation and processing of this zymogen is a highly specific and controlled process. It was also shown that the connecting region conformation has an influence in the kinetics of pro-CPB activation.

In this work, additional mutants have been studied to evaluate the relevance of the tryptic targets in more detail and to determine the structural features that cause the different behaviour of the A1 and B forms upon activation. The main objective of this work is to complete the detailed description of the structural/functional relationships in the activation/inhibition mechanisms of pancreatic procarboxypeptidase B.

## 1.3. Materials and Methods

### 1.3.1. Materials

Restriction enzymes, T4 DNA ligase, *Taq* polymerase, deoxyribonucleotide stocks and synthetic oligonucleotides were obtained from Roche Molecular Biochemicals. Vent DNA polymerase was purchased from New England Biolabs. Salts and mediums for *Escherichia coli* and *Pichia pastoris* were purchased from Difco. The *Pichia pastoris* strains and vectors were obtained from Invitrogen. Trypsin (treated with tosyl-L-phenyl chloromethyl ketone) was from Worthington.  $N^{\alpha}$ -*p*-tosyl-L-lysine chloromethyl ketone and benzoylglycyl-L-arginine (BGA) were from Sigma.

### 1.3.2. Site-directed mutagenesis by PCR

Site-specific mutations were introduced by a two-step PCR procedure using 5'-GGGAGCATTCTGAAGGGAAAAGGTGTTCCGTGTC as sense external primer (a silent Asp700 site elimination serves for recombinant screening) and 5'-

TCTCTCACTTCCTCTGGCAAAATGCATGGGAAAT as antisense external primer. In order not to introduce so many mutations by PCR, different previously made vectors that contained the pre-pro  $\alpha$ -mating factor ( $\alpha$ -MF) and the pro-CPB gene with different mutations were used as templates. The sequence of these constructs (named PGLD22, 24, 26 and 28) is compared to the wild type pro-CPB sequence in figure 1.1. The pairs of internal primers used for the first step of PCR are also represented in figure 1.1 and the mutations introduced in each case are indicated. The different resulting DNA fragments containing the pre-pro  $\alpha$ -MF plus the newly mutated pro-CPB were cloned into the *Bam*H1 site of pPIC 3.5 to obtain pPIC3.5-VC1 to VC4. All the constructs were confirmed by sequencing on an automated DNA sequencer.

### Primers for pVC2: mutant R83Q/R93Q

	83												93											
Wild type pro-CPB	N	L	R	S	V	L	E	A	Q	F	D	S	R	V	R	T	T	G	H	S	Y			
PGLD 24	N	L	Q	S	V	L	E	A	Q	F	D	S	R	V	R	T	T	G	H	S	Y			
	AAC	CTG	CAG	TCT	GTG	CTC	GAG	GCT	GAG	TTT	GAC	AGC	AGA	GTC	CGT	ACA	ACT	GGA	CAC	AGT	TAT			
Mutations	Q																							
	TT GAC AGC CAA GTC CGT ACA ACT GGA CAC AGT TAT CAA GCG CTC CGA GCT AAA CTG TCG GTT CAG GCA TG																							

### Primers for pVC3: mutant R93Q/R95Q/T97R

	2														
Wild type pro-CPB	F	D	S	R	V	R	T	T	G	H	S	Y	E	K	Y
PGLD 28	F	D	S	Q	V	Q	T	T	G	H	S	Y	E	K	Y
	TTT	GAC	AGC	CAA	GTC	CAG	ACA	ACT	GGA	CAC	AGT	TAT	GAG	AAG	TAC
Mutations	R														
	C CAG ACA AGA GGA CAC AGT TAT GAG AAG CTG TCG GTT CAG GTC TGT CCT GTG														

### Primers for pVC1: mutant $\alpha_3$ helix

	83												93											
Wild type pro-CPB	I	N	N	L	R	S	V	L	E	A	Q	-	-	-	-	-	F	D	S	R	V	R	T	
PGLD22	I	N	N	L	R	S	V	L	E	A	E	Q	E	Q	M	F	A	S	Q	G	R	T		
	ATA	AAC	AAC	CTG	AGA	TCT	GTG	CTC	GAG	GCT	GAG	CAG	GAG	CAG	ATG	TTT	GCC	AGC	CAG	GGC	CGT	AC		
Mutations	E D Q L D E A																							
	G CAA TCT CTG CTC GAC GAA GAG CAG GAG CAG GCC TTT GCC AGC CAG GGC CG GAT GTT ATA CTC CAT GAG TAT CTC CTG GAC GTT AGA GAC GAG CTG CTT C																							

### Primers for pVC4: mutant $\beta_{10}$ helix

	41																					
Wild-type pro-CPB	Q	I	D	F	W	K	P	D	S	V	T	Q	I	D	P	H	S	T	V	D		
PGLD 26	K	P	D	S	-	-	-	-	-	-	-	K	P	H	S	T	V	D				
	GG	CAG	ATT	GAC	TTC	TGG	AAA	CCA	GAT	TCT	---	---	---	---	---	AAA	CCT	CAC	AGT	ACA	GTT	GAC
Mutations	G P A R																					
	C TGG AAA GGA CCT GCT --- --- --- --- AGA CCT CAC AGT ACA GTT GAC CC GTC TAA CTG AAG ACC TTT CCT GGA CGA --- --- --- --- TCT GGA GTG																					

Figure 1.1 Internal primers for the first step of PCR in the construction of the different mutants.

### 1.3.3. Transformation and selection of productive clones

The different expression vectors containing the mutated pro-CPB cDNAs (pPIC-VC1 to VC4) were linearized by *SacI* digestion and transformed into *P. pastoris* KM71 (*arg4*, *his4*, *aox1::ARG4*) strain by the spheroplast method. Histidine-independent transformants were selected. Colonies were grown in a buffered liquid medium BMGY and BMMY (1% yeast extract, 2 % peptone, 90 mM potassium phosphate, pH 6.0, 1.34% yeast nitrogen base,  $4 \times 10^{-5}$  biotin, and either 1% glycerol or 0.5% methanol) using 10-ml test cultures at 30 °C for 5 days. The production of the clones was followed by SDS-polyacrylamide gel electrophoresis on 12% acrylamide gels. The functionality of the expressed protein was analyzed with the synthetic substrate BGA after activation of the proenzyme with trypsin (at a 1:1 ratio by weight).

### 1.3.4. Expression and purification of pro-CPB mutants

One-litre shake-flask cultures were grown for 3 days in buffered glycerol medium BMGY (15-20 OD units at 600 nm). Cells were collected by centrifugation at 1500 g, gently re-suspended in 200 ml of the methanol-containing medium BMMY and cultured for another 2 days to induce the production of the protein. The supernatant was loaded onto a hydrophobic interaction butyl column and eluted with a decreasing gradient of ammonium sulfate. The zymogen-containing fractions were selected for their activity against BGA after tryptic activation and re-purified by fast protein liquid chromatography on an anion exchange column (TSK-DEAE) as reported previously (Villegas *et al.*, 1995). The culture medium was dialyzed against the activation buffer (50 mM Tris-HCl, 1µM ZnCl<sub>2</sub>, pH 7.5) and concentrated to 0.2 ml by ultra-filtration (Amicon).

### 1.3.5. Proteolytic processing of the recombinant proenzymes

The recombinant proenzymes at 1mg/ml in activation buffer were treated with trypsin at 400/1 ratio (w/w) at 0 °C. At given times after trypsin addition, aliquots were removed for activity measurements, electrophoretic analysis and reverse-phase HPLC

analysis. For activity measurements, 10 µl of the activation mixture were mixed with 190 µl of aprotinin at 0.1 mg/ml in 20 mM Tris, 0.1 M NaCl, pH 7.5, and 10 µl of this new mixture were used to carry out spectrophotometric activity measurements with BGA at 254 nm. For electrophoretic analysis, 2 µl of  $N^{\alpha}$ -*p*-tosyl-L-lysine chloromethyl ketone at 22 mM in water were added to 20 µl of the activation mixture to reach a final trypsin inhibitor concentration of 2 mM. Each sample was immediately mixed with electrophoretic loading buffer (containing 1% SDS and 3%  $\beta$ -mercaptoethanol), heated at 90 °C for 1 min, and stored at –20 °C until analyzed. Electrophoresis was carried out in polyacrylamide Tricine gels (Schägger *et al.*, 1987). For HPLC analyses, 90-µl samples were removed from the activation mixture, adjusted to 0.5% trifluoroacetic acid to inhibit proteolysis, and immediately chromatographed or kept at –20 °C for subsequent analysis.

### **1.3.6. Chromatographic analysis and purification of the activation products**

Samples removed from the activation mixtures were analyzed by reversed-phase HPLC on Vydac C4 supports. A 214TP54 column, 250 x 4.6 mm, 5-µm particle size, 0.3-µm pore was used, and chromatographies were performed in 0.1% trifluoroacetic acid with a linear elution gradient between water (solvent A) and acetonitrile (solvent B), according to the following steps: 10% B from 0 to 10 min and 52% B at 130 min.

## 1.4. Results and discussion

### 1.4.1. Overexpression in yeast, Purification and Characterization of the different mutants of Pro-CPB

The recombinant plasmids containing the different mutated sequences (pPIC3.5-VC1 to -VC4) and the one containing the wild type pro-CPB sequence were linearized by *SacI* digestion and used to transform the KM71 (*arg4*, *his4*, *aox1::ARG4*) *P. pastoris* strain by the spheroplast method. Transformed cells were screened for pro-CPB secretion, and the selected clones were used for large scale productions of the different pro-CPB mutants. The cells were first grown in the presence of glycerol and then switched to methanol (1%) as the carbon source to induce expression of pro-CPB.

Starting from 200 ml of culture medium, the two-step chromatographic method used to purify the mutants of pro-CPB normally yielded an average quantity of 10 mg of protein.

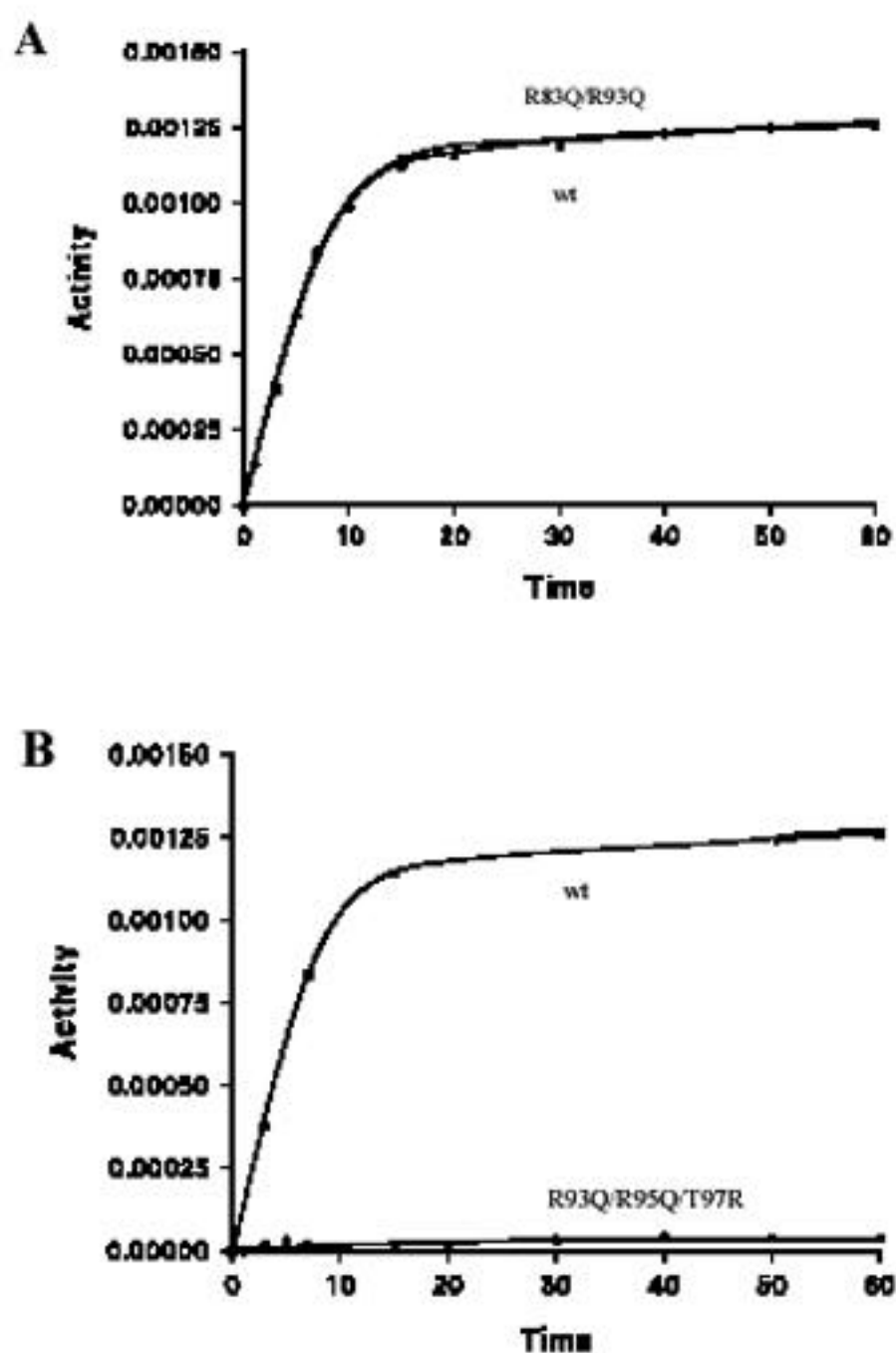
### 1.4.2. Mapping Tryptic Targets in Pro-CPB-Connecting Segment

In pro-CPB, the globular domain of the pro-segment is connected to the enzyme by a two-turn  $\alpha$ -helix followed by a nonstructured flexible loop (Coll *et al.*, 1991). This connecting region contains three Arg at positions 83, 93 and 95. Although all of them appear to be solvent-exposed, the first tryptic cleavage of the proteolytic processing of pro-CPB occurs only at Arg 95. This initial cut is followed by the trimming of the pro-segment C-terminal residue by the generated CPB. A second tryptic cleavage occurs at the Arg 83 – Ser 84 bond in the N-terminal region of the  $\alpha$ -helix. Previous studies have shown that Arg 93 may also act as primary tryptic target when carboxypeptidase inhibitors are added to the activation mixture (Villegas *et al.*, 1995).

In a previous work (Ventura *et al.*, 1999), different mutants were produced in order to individualize the effect of the different tryptic targets. It was shown that, although Arg 95 is normally the initial target for proteolytic processing, Arg 93 can also take this role in the absence of Arg 95 and under strong activation conditions (25 °C and 4/1 pro-CPB/trypsin ratio). When both Arg 93 and 95 are absent, there is no conversion of pro-CPB into active enzyme even under strong proteolytic conditions.

In this work, two new mutants on the tryptic targets have been studied: a double mutant R83Q/R93Q and the triple mutant R93Q/R95Q/T97R. Tryptic activation of the double mutant generates full CPB activity at a rate similar to that of the wild-type enzyme (Figure 1.2A), indicating that the absence of a secondary (Arg83) or alternative (Arg93) tryptic target has no effect on the kinetics of the process. This behaviour is very similar to that of the single mutant R83Q previously analyzed. However no biphasic behaviour in the activation course is detected in this case at short times after trypsin addition, in contrast to the observations made with the single R83Q mutant (Ventura *et al.*, 1999). In the latter case, the slight deceleration of the activation course (as measured by generation of carboxypeptidase activity) was correlated with the levels of primary activation segment (1-95) present in the activation mixture. If that was the case, the same effect should have appeared, and even more clearly, in the double mutant as the complete activation segment (1-95) is expected to be produced in this case. The absence of delay in the appearance of activity confirms that, however long the activation fragments released from pro-CPB are, they do not have the ability to inhibit the enzyme in the isolated state. This points out to the important contribution of the connecting segment to the positioning of the globular activation domain onto the enzyme moiety, thus allowing the inhibitory action to take place. The discrepancy between the single and double mutants must then be ascribed to the additional mutation R93Q, which may add some instability to the connecting region by eliminating positive charges that stabilize the C-terminal of helix 3 and render this region less stable and even less prone to interact with the enzyme domain. The conversion rate of pro-CPB into CPB also appears to be similar to the wild type enzyme when the activation process is analyzed by SDS electrophoresis (figure 1.3), although a slight delay in the complete appearance of CPB may be observed, possibly as a result of conformational changes due to the previously commented additional mutation R93Q, which may also render the primary tryptic target less accessible to trypsin. A clear difference between this mutant and the wt form is obviously observed through the analysis of the generated fragments by HPLC: degradation of the activation segment does not proceed further than Val94 at 40 min

activation time due to the absence of the second tryptic target (figure 1.4A). It must be recalled here that CPB is very inefficient in digesting residues other than Arg when the substrates are its own activation segments (Villegas *et al.*, 1995). As a result of the absence of Arg93, the fragment 84-94, a major degradation product in wt pro-CPB activation, is not generated in this mutant.



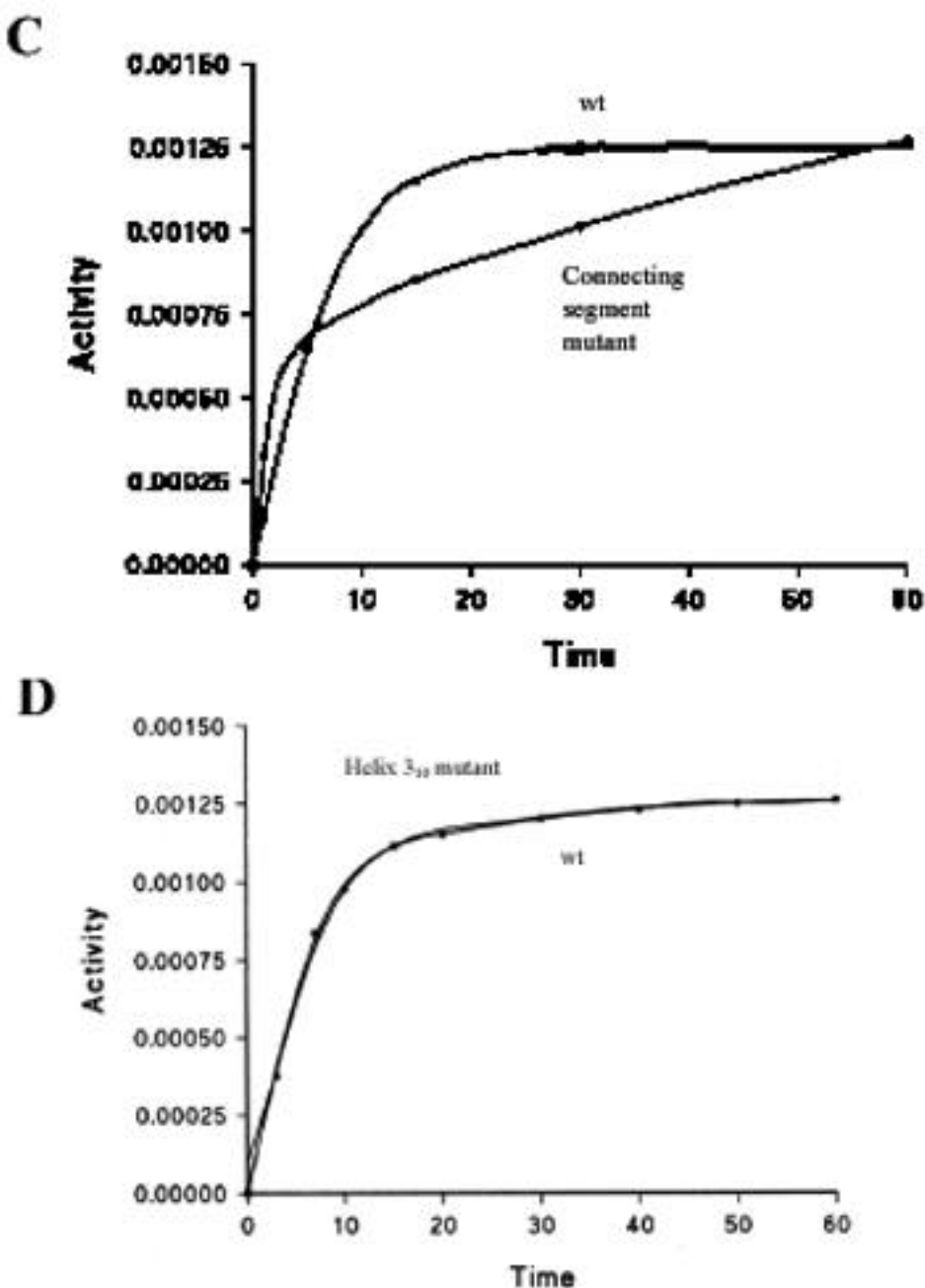


**Figure 1.2. Comparison of the time course of CPB activity generation after trypsin activation in wild-type and mutant pro-CPBs.** Recombinant pro-CPBs at 1 mg/ml in 50mM Tris-HCl, 0.01 mM ZnCl<sub>2</sub> (pH 8.0) were treated with trypsin as indicated, and at controlled times, aliquots were withdrawn and analyzed for carboxypeptidase B activity using 1 mM BGA as substrate. The activity is measured in mMols/mg min and the time is measured in minutes. The graphics correspond to the following mutants: A, connecting segment mutant; B, R83Q/R93Q; C, R93Q/R95Q/T97R; D, inhibitory region mutant

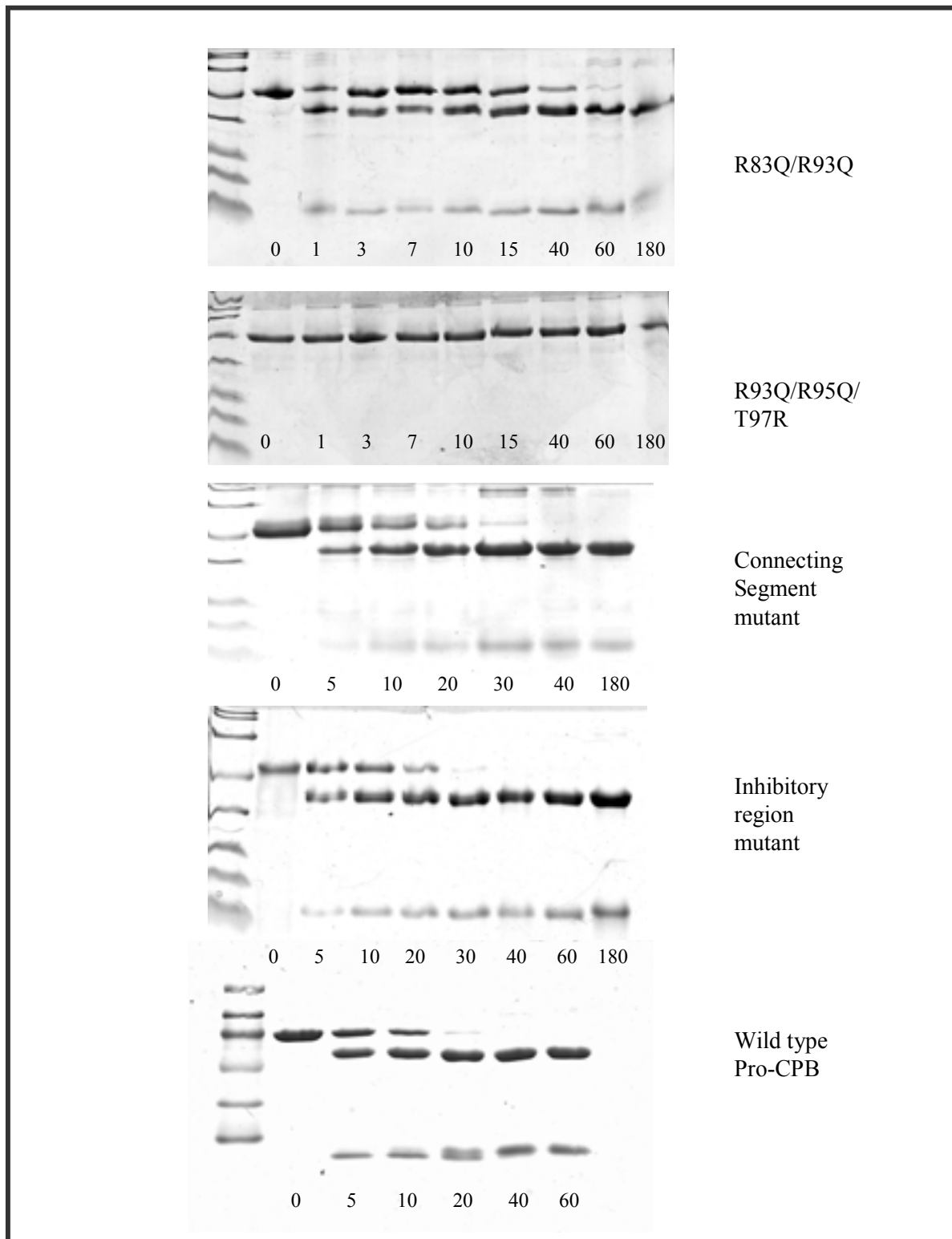
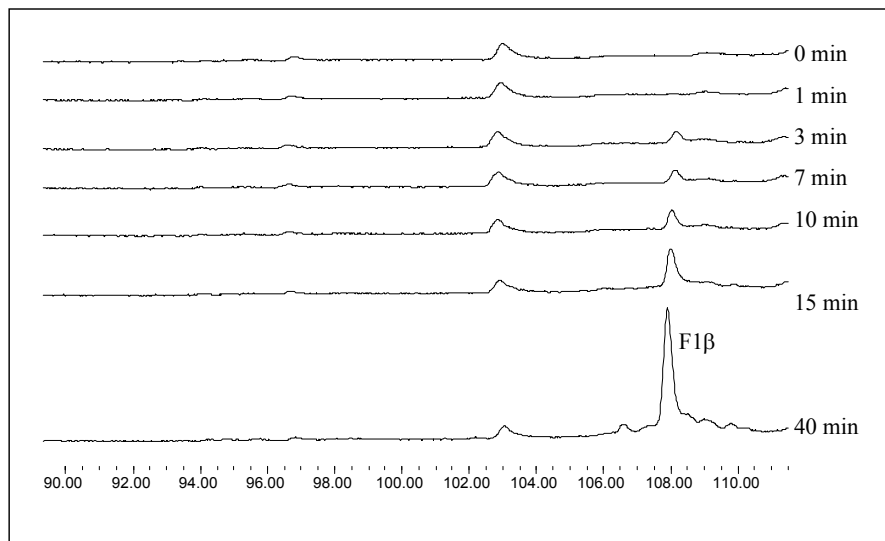


**Figure 1.3. Electrophoretic analysis of the proteolytic processing of pro-CPB by trypsin.** The recombinant wild type and mutant proenzymes at 1 mg/ml in the activation buffer were treated with trypsin at 400:1 ratio (w:w) at 0 °C. At given times after trypsin addition, aliquots were removed, made 1 mM in N<sup>α</sup>-p-tosyll-l-lysine chloromethyl ketone, mixed with loading buffer, heated at 100 °C and stored at –20 °C until analysis.

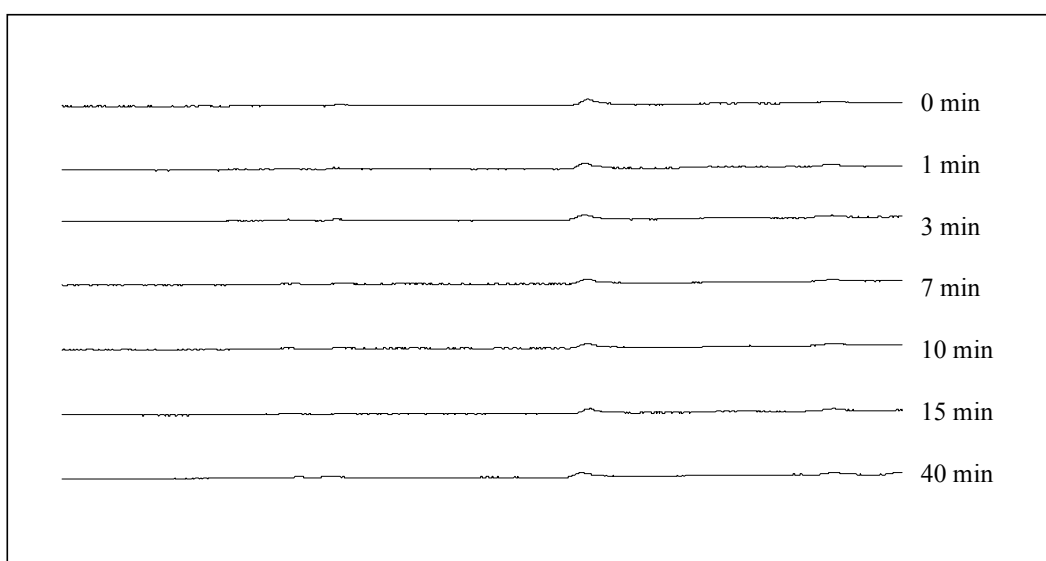
In the triple mutant, the tryptic targets at positions 93 and 95 were eliminated and a new tryptic target was created at position 97, mimicking the targets pattern that exists in pro-CPA1. This mutant is not activatable with trypsin under standard activation conditions for pro-CPB (figure 1.2B). The electrophoretic and HPLC analysis shows that there is no conversion of pro-CPB into CPB through time after trypsin addition (figures 3 and 4B). The study of this mutant indicates that either Arg 95 or Arg 93 are necessary for the activation of pro-CPB and that the function of these residues cannot be taken as by an artificial target placed in position 97. Pro-CPA 2 has its primary activation site (Arg99) at a position sequentially equivalent to the engineered Arg97 in PCPB. However, as the respective 3D structures show (Coll *et al.*, 1991; García-Sáez *et al.*, 1997), the location of those residues and their exposure to solvent and activating proteases are fairly different: Arg 99 is located at the end of the long connecting helix, and is the most exposed residue of all possible basic activation targets, whereas the engineered Arg97 in pro-CPB is in the middle of the loop that turns “backwards” to the enzyme moiety, making it less prone to accept a tryptic attack. Thus, the arrangement of the activation targets at the connecting regions of pro-CPs seems to follow an individual pattern for each form of the proenzymes.

A

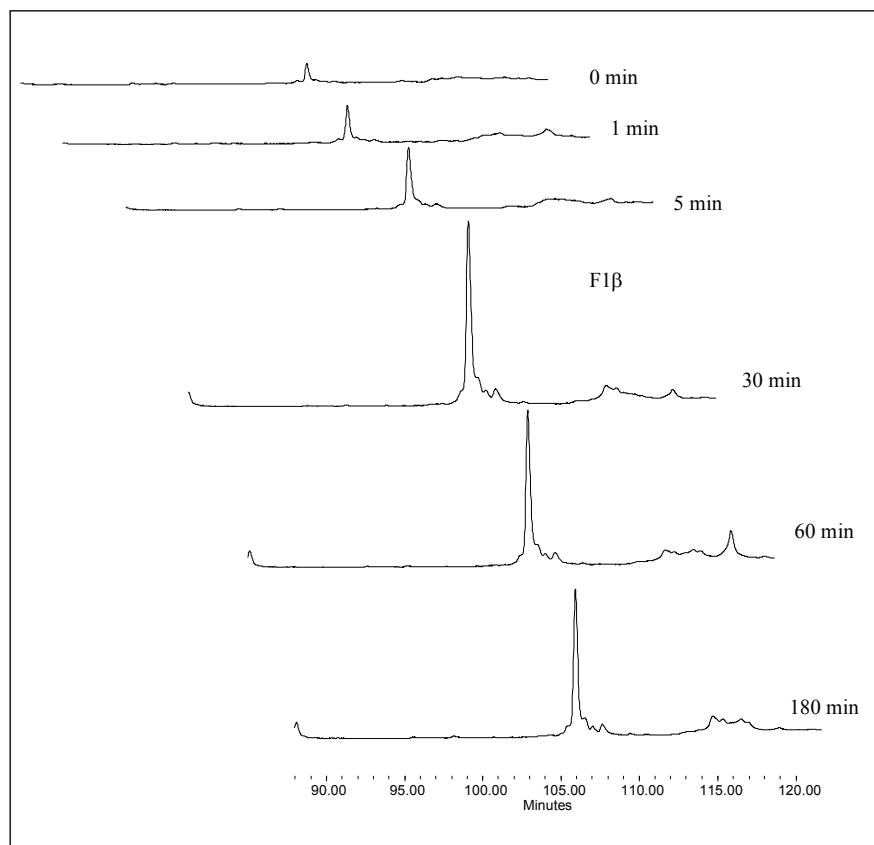


R83Q/R93Q

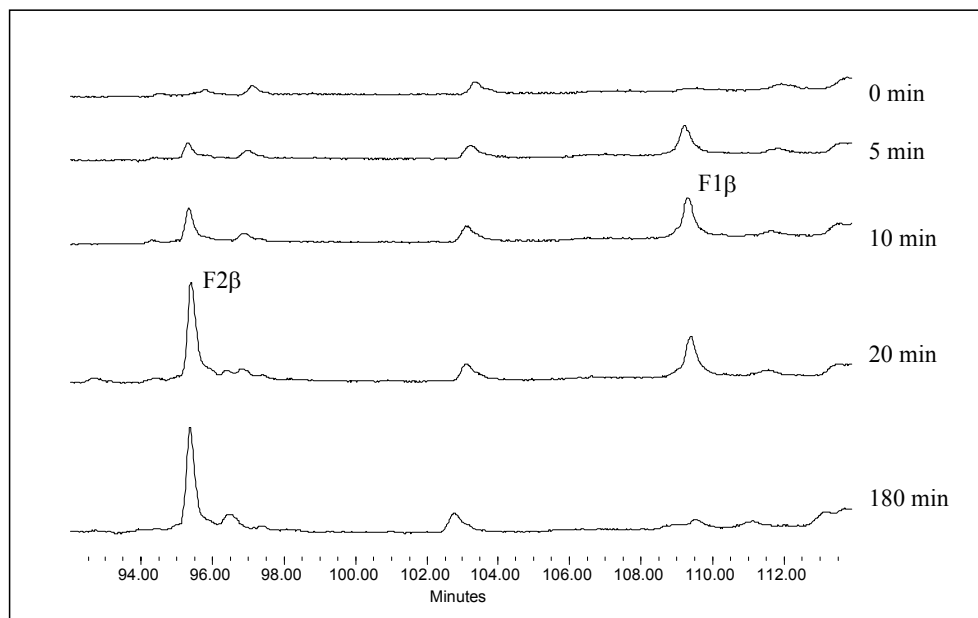
B



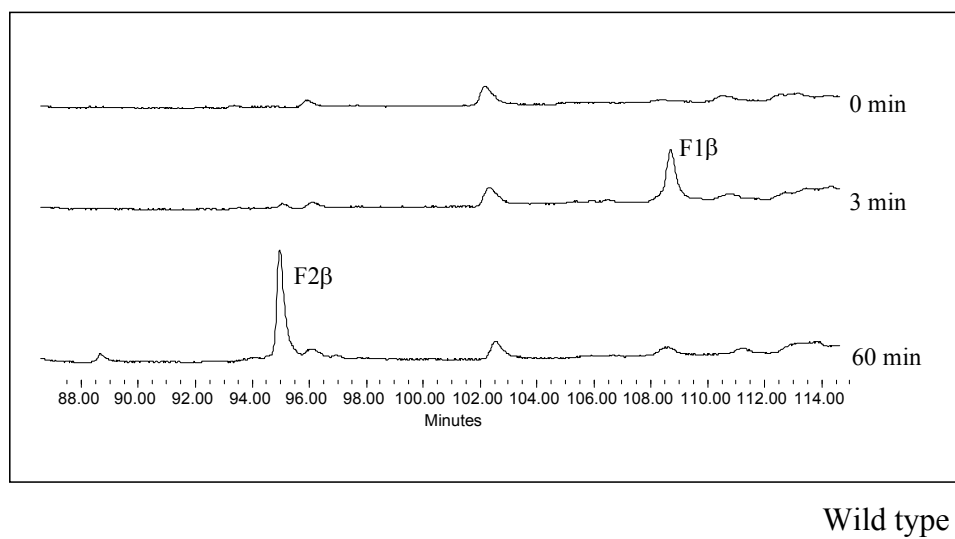
R93Q/R95Q/T97R

**C**

Connecting segment mutant

**D**

Inhibitory region mutant

**E**

**Figure 1.4. Comparative analysis of the fragments generated during tryptic processing of recombinant pro-CPB by reversed phase HPLC.** At different times after trypsin addition, aliquots were taken from the activation mixture in the same conditions as in figure 1.3 and analyzed by reversed phase chromatography on an HPLC system. The action of trypsin was stopped by adding trifluoroacetic acid up to 0.1%. 15 µl of each sample were loaded on a Vydac C4 reversed phase column. The different profiles correspond to the following proteins: A, connecting segment mutant; B, R83Q/R93Q; C, R93Q/R95Q/T97R; D, inhibitory region mutant; E, wild type pro-CPB.

#### 1.4.3. Relevance of the Connecting Segment in the Pro-CPB Tryptic Activation

The connecting segment of the pro-CPB shows a number of differences compared to the corresponding region in pro-CPA1. While in pro-CPB there is a hydrogen bond between Gln 89 and Arg 124 of the active enzyme, the equivalent residues in pro-CPA1 –Glu 89 and Arg 124- form a strong saline bridge (Avilés *et al.*, 1993). In addition, the  $\alpha$ 3 helix is only two turns long in pro-CPB versus the four turns of pro-CPA1. The longer helix of pro-CPA1 seems to be responsible for maintaining the interaction between the pro-region and the carboxypeptidase after tryptic action (Vendrell *et al.*, 1993). The lack of inhibitory ability shown by the pro-region of CPB could be explained through the following reasons: a lower number of contacts between the helix and the active enzyme, the weakness of a hydrogen

bond compared to a salt bridge and the fact that a short helix with few internal contacts tends to lose its structure in the absence of covalent continuity in the polypeptidic chain. To test the relevance of the specific properties of the connecting segment in the differences between the activation processes of pro-CPB and pro-CPA1, pro-CPB mutant was designed in a way that the whole connecting segment of pro-CPB was substituted by the longer helix present in pro-CPA1. The protein sequence of this mutant, compared to those of pro-CPB and pro-CPA1, is represented in figure 1.5. Three point mutations were also introduced to increase the helical propensity and the final design was tested by the AGADIR software for helicity prediction (Muñoz and Serrano, 1995). In wild type pro-CPA1, the fragment comprised by the residues I 79 and R 99 has a TPH (total peptide helicity) value of 2.73 %, expressed as the % of peptide molecules that adopt a helix  $\alpha$  conformation in solution, whereas in the corresponding fragment of the mutant, the TPH value was calculated to be 3.68 %.

Pro-CPA1 sequence	I E D V Q L L D E E Q E Q M F A S Q G R A R T
Pro-CPB sequence	I N N L R S V L E A Q - - - F D S R V R T T G
Mutant sequence	I E D L Q S L L D E E Q E Q A F A S Q G R T T G

**Figure 1.5. Comparison of the sequence of the connecting segment mutant with those of pro-CPA1 and pro-CPB.**

Analysis of the activation process of the connecting segment mutant shows that the generation of activity along time is slowed down as compared to the wild type pro-CPB (figure 1.2C). Electrophoretic analysis shows that the release of mature enzyme follows the same rate observed in the wild type (figure 1.3). As expected, and as analysed by SDS electrophoresis and HPLC (figure 1.4C), there is no conversion of fragment F1 (1-95,94) into F2 (1-83,82) or F3 (1-81) because of the absence of the secondary target R83. The major product of the activation is fragment F1 $\beta$  (1-94), generated by carboxypeptidase action on the C-terminal arginine of the primary activation segment. Thus, the effect on the kinetics of carboxypeptidase activity generation should be related to the presence of this form of activation segment in the reaction mixture.

The rate of activity generation is in this case clearly slowed down in comparison to the previously commented mutants R83Q and R83Q/R93Q, which were also devoid of the secondary tryptic target. However, the behaviour of the mutant reproduces neither the long-lasting persistence of inhibitory action shown by pro-CPA1 activation segment nor the biphasic behaviour of the A1 zymogen activation. Pro-CPB is thus not able to reproduce the activation process of pro-CPA1 by simply substituting its connection segment.

From the comparison of these results with those obtained from the point and double mutants commented upon previously, it can be deduced that it is not only the covalent integrity of the released activation segment but also, and in the first place, its overall structure and stability and its capacity to bond to complementary surfaces on the active enzyme which are responsible for inhibitory action of the carboxypeptidase moiety. In the design of this mutant care was taken to maintain the local helical structure of the connecting segment. However, the effect of the mutations introduced has not been theoretically previewed by means of docking of complementary surfaces at the interface of both moieties or by molecular modeling. This approach, much more demanding in terms of design and experimental test, is probably advisable when trying to modify a molecular behaviour in which aspects of local and global structure and stability are involved.

#### 1.4.4. Determinants of pro-CPB Inhibition

In porcine pro-CPB, the pro-region sequence located over the active site cleft of the enzyme is formed by part of the  $\beta$ 2 strand, a cis-proline turn and one turn of  $3_{10}$  helix, with an aspartate at position 41 located after the cis-proline. This aspartate forms a salt bridge with Arg 145 in the enzyme, a residue that, in the absence of the pro-segment, binds to the C-terminal carboxyl group of substrate molecules. This interaction might partially explain the null intrinsic activity in pro-CPB against small peptide substrates (Avilés *et al.*, 1993). By contrast, porcine pro-CPA1 is able to hydrolyze substrates before it is activated. This activity accounts for 10% of the  $V_{max}$  for small substrates and 1% for hexapeptides (Serra *et al.*, 1992). In the A forms, intrinsic activity is due to a pre-formed active site in the zymogen and to the diffusion ability of the substrates towards this active site through cavities between the surfaces of the protein domains (García-Sáez *et al.*, 1997).

To test the relevance of the sequence and secondary structure elements in this different behaviour between pro-CPB and the A forms, the ‘inhibitory region’ of pro-CPB was replaced by the corresponding region of pro-CPA1. The sequence PDSVTQIK in pro-CPB, containing Asp41 and the  $\beta_{10}$  helix turn, was substituted by the A1 sequence GPAR, devoid of any of those elements. The mutant has thus a shorter sequence and is not able to form a salt bridge with Arg145 in the enzyme domain.

Expression of these mutants was more satisfactory than previously assayed ones (Ventura *et al.*, 1999) in which only a  $\beta_{10}$  helix deletion, but not a B/A1 sequence substitution had been performed, although the levels of purified protein were lower than for the rest of the mutants.

Intrinsic activity and total CPB activity after tryptic activation were measured on small synthetic peptide substrates immediately after the second purification step. An excess of potato carboxypeptidase inhibitor was added to the solution when testing intrinsic activity to avoid detection of active enzyme traces. The results are represented in figure 1.6. The mutant shows detectable values of intrinsic activity compared to the null activity of wild-type pro-CPB, but still not as high as those of the A forms, that can reach 10% of total potential CPA activity. In terms of activity generation rate and HPLC follow-up of the activation mixture, this mutant showed a behaviour identical to wild type pro-CPB (figures 2D, 3 and 4D).

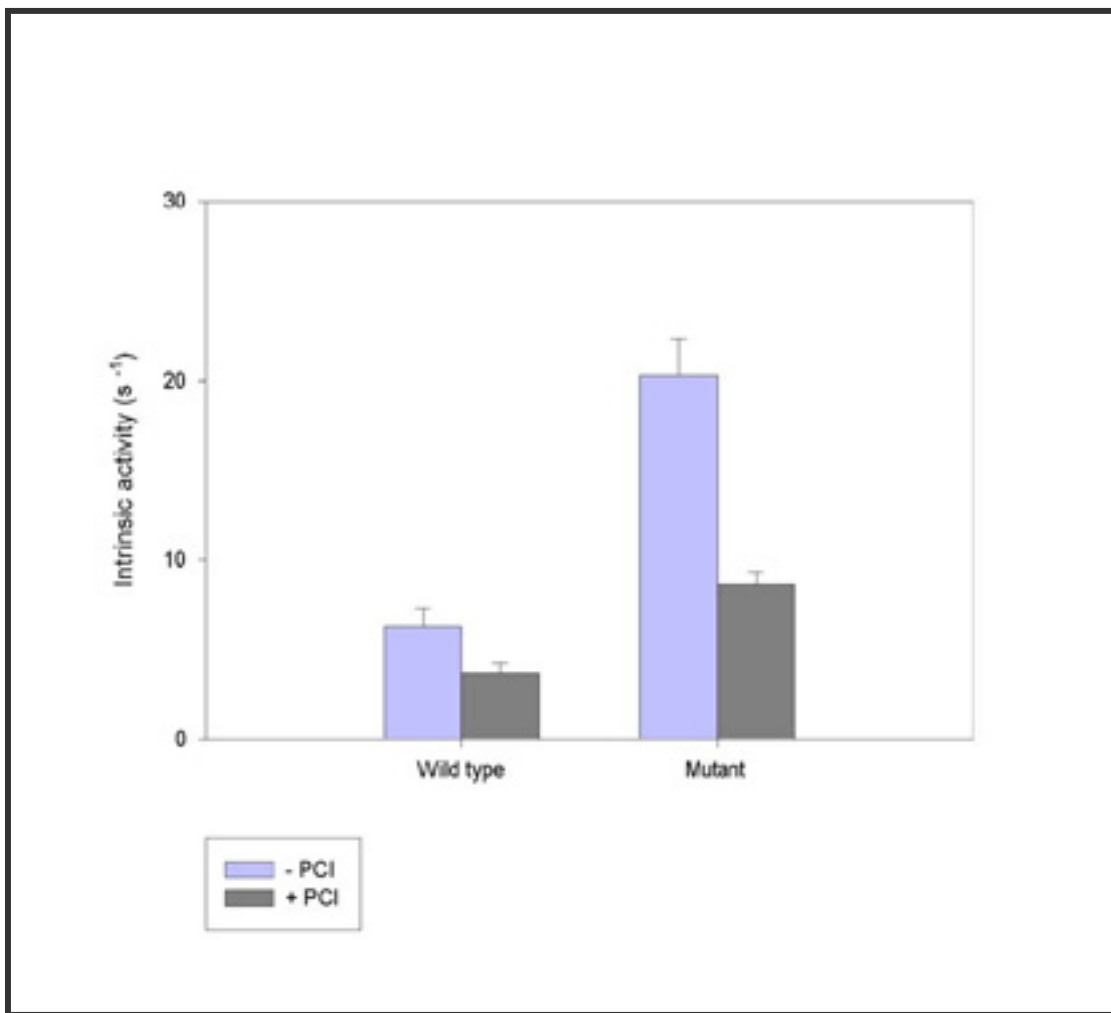


Figure 1.6. Intrinsic activity of the inhibitory region mutant compared to the wild type.

## 1.5. References

- Aloy P, Catasús L, Villegas V, Reverter D, Vendrell J, Avilés FX (1998) Comparative analysis of the sequences and three-dimensional models of human procarboxypeptidases A1, A2 and B. *Biol Chem Hoppe-Seyler* 379, 149-155.
- Avilés FX, Vendrell J, Guasch A, Coll M, Huber R (1993) Advances in metallo-procarboxypeptidases. Emerging details on the inhibitory mechanism and on the activation process. *Eur J Biochem* 211, 391-399.
- Burgos FJ, Salvà M, Villegas V, Soriano F, Méndez E, Avilés FX (1991) Analysis of the activation process of porcine procarboxypeptidase B and determination of the sequence of its activation segment. *Biochemistry* 30, 4092-4099.
- Coll M, Guasch A, Avilés FX, Huber R (1991) Three-dimensional structure of porcine procarboxypeptidase B *EMBO J* 9, 1-9.
- García-Sáez I, Reverter D, Vendrell J, Avilés FX, Coll M (1997) The three dimensional structure of human procarboxypeptidase A2. Deciphering the basis of the inhibition, activation and intrinsic activity of the zymogen. *EMBO J* 16, 6906-6913.
- Guasch A, Coll M, Avilés FX, Huber R (1992) Three-dimensional structure of porcine pancreatic procarboxypeptidase A. A comparison of the A and B zymogens and their determinants for inhibition and activation. *J Mol Biol* 224, 141-157.
- Lacko AG, Neurath H (1970) Studies on procarboxypeptidase A and carboxypeptidase A of the spiny pacific dogfish (*Squalus acanthias*). *Biochemistry* 9, 4680-4690.
- Muñoz V, Serrano L (1995) Elucidating the folding problem of helical peptides using empirical parameters. *J Mol Biol* 245, 275-296.
- Neurath H (1986) The versatility of proteolytic enzymes. *J Cell Biochem* 32, 35-49.

Reeck GR, Neurath H (1972) Isolation and characterization of PCPB and CPB of the African lungfish. Biochemistry 11, 3947-3955.

Schägger H, Von Jagow G (1987) Tricine-sodium dodecyl sulfate-polyacrilamide gel electrophoresis for the separation of proteins in the range from 1 to 100 kDa. Anal Biochem 166, 368-379.

Serra MA (1995) Study of the Peptide Hydrolysis Kinetics of Carboxypeptidase A. Ph.D. thesis, Universitat Autònoma de Barcelona.

Vendrell J, Cuchillo CM, Avilés FX (1990) The tryptic activation pathway of monomeric procarboxypeptidase A. J Biol Chem 265, 6949-6953.

Vendrell J, Billeter M, Wider G, Avilés FX, Wüthrich K (1991) The NMR structure of the activation domain isolated from porcine procarboxypeptidase B. EMBO J 10, 11-15.

Vendrell J, Catasús Ll, Opezzo O, Ventura S, Villegas V, Avilés FX (1993) Ed. Walter de Gruyter. Berlin, NY. Chapter 16, 279-297.

Ventura S, Villegas V, Sterner J, Larson J, Vendrell J, Hershberger CL, Avilés FX (1999) Mapping the pro-region of carboxypeptidase B by protein engineering. Cloning, overexpression and mutagenesis of the porcine proenzyme. J Biol Chem 274, 19925-19933.

Villegas V, Vendrell J, Avilés FX (1995) The activation pathway of procarboxypeptidase B from porcine pancreas: participation of the active enzyme in the proteolytic processing. Protein Sci 4, 1792-1900.